

AD-A103 347 NATIONAL AVIATION FACILITIES EXPERIMENTAL CENTER ATL--ETC F/6 1/2
AIRBORNE RADAR APPROACH.(U)
APR 80 C MACKIN

UNCLASSIFIED FAA-NA-79-56

FAA-RD-A0-22

NL

1 OF 1
40 A
DIA8347

END
DATE PRINTED
10-81
DTIC

Report No. FAA-RD-80-22

LEVEL

(1)

ADA103347

AIRBORNE RADAR APPROACH

C. Mackin



FINAL REPORT

APRIL 1980

Document is available to the U.S. public through
the National Technical Information Service,
Springfield, Virginia 22161

Prepared for

U. S. DEPARTMENT OF TRANSPORTATION
FEDERAL AVIATION ADMINISTRATION
Systems Research & Development Service
Washington, D. C. 20590

81825116

b7d FILE COPY

64-871

NOTICE

The United States Government does not endorse products or manufacturers. Trade or manufacturer's names appear herein solely because they are considered essential to the object of this report.

Technical Report Documentation Page

1. Report No. FAA-RD-80-22	2. Government Accession No. AD-4103547	3. Recipient's Catalog No.	
4. Title and Subtitle AIRBORNE RADAR APPROACH	5. Report Date April 1980		
6. Author(s) C. Mackin	7. Performing Organization Code		
8. Performing Organization Name and Address Federal Aviation Administration National Aviation Facilities Experimental Center Atlantic City, New Jersey 08405	9. Performing Organization Report No. FAA-NA-79-56		
10. Work Unit No. (TRAIS)	11. Contract or Grant No. 045-390-130		
12. Sponsoring Agency Name and Address U.S. Department of Transportation Federal Aviation Administration Systems Research and Development Service Washington, D.C. 20590	13. Type of Report and Period Covered Final Report September 1978-February 1979		
14. Sponsoring Agency Code			
15. Supplementary Notes			
16. Abstract A flight test series investigating the airborne radar approach (ARA) for helicopters is discussed. Passive and active target enhancement methods and their relative merits are examined. A description of systems and methods involved in the ARA are presented along with subjective insights and conclusions. It is concluded that the ARA is a practical approach aid in the absence of conventional navigation aids (NAVAID's) subject to certain limitations as discussed herein.			
17. Key Words Helicopter Instrument Flight Rules Weather Radar Transponder Beacon Offshore Corner Reflector		18. Distribution Statement Document is available to the U.S. public through the National Technical Information Service, Springfield, Virginia 22161	
19. Security Classif. (of this report) Unclassified	20. Security Classif. (of this page) Unclassified	21. No. of Pages 46 43	22. Price



METRIC CONVERSION FACTORS

Approximate Conversions to Metric Measures

Symbol	When You Know	Multiply by	To Find	Symbol
<u>LENGTH</u>				
in	inches	.75	centimeters	cm
ft	feet	.30	centimeters	cm
yd	yards	.9	meters	m
mi	miles	1.6	kilometers	km
<u>AREA</u>				
in ²	square inches	6.5	square centimeters	cm ²
ft ²	square feet	0.09	square meters	m ²
yd ²	square yards	0.8	square meters	m ²
mi ²	square miles	2.6	square kilometers	km ²
	acres	0.4	hectares	ha
<u>MASS (weight)</u>				
oz	ounces	.28	grams	g
lb	pounds	.45	kilograms	kg
	short tons	.9	tonnes	t
	(2000 lb.)			
<u>VOLUME</u>				
teaspoon	5	milliliters	ml	
tablespoon	15	milliliters	ml	
fluid ounces	30	milliliters	ml	
cup	.24	liters	l	
pint	.47	liters	l	
quart	.95	liters	l	
gallon	3.8	liters	l	
cubic foot	.03	cubic meters	m ³	
cubic yards	.76	cubic meters	m ³	
<u>TEMPERATURE (exact)</u>				
°F	Fahrenheit temperature	5/9 (after subtracting 32)	Celsius temperature	°C

Approximate Conversions from Metric Measures

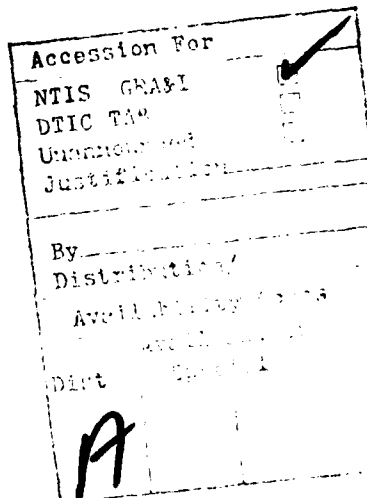
Symbol	When You Know	Multiply by	To Find	Symbol
<u>LENGTH</u>				
mm	millimeters	0.04	inches	in
cm	centimeters	0.4	inches	in
m	meters	3.3	feet	ft
km	kilometers	1.1	feet	ft
		0.6	yards	yd
			miles	mi
<u>AREA</u>				
cm ²	square centimeters	0.16	square inches	in ²
m ²	square meters	1.2	square yards	yd ²
km ²	square kilometers	0.4	square miles	mi ²
	hectares (10,000 m ²)	2.5	acres	ac
<u>MASS (weight)</u>				
g	grams	0.036	ounces	oz
kg	kilograms	2.2	pounds	lb
t	tonnes (1000 kg)	1.1	short tons	lb
<u>VOLUME</u>				
ml	milliliters	0.03	fluid ounces	fl oz
l	liters	2.1	pints	pt
l	liters	1.06	quarts	qt
m ³	cubic meters	0.26	gallons	gal
m ³	cubic meters	35	cubic feet	ft ³
m ³	cubic meters	1.3	cubic yards	yd ³
<u>TEMPERATURE (exact)</u>				
°C	Celsius temperature	5/9 (then add 32)	Fahrenheit temperature	°F

* 1 m = 3.28 feet; 1 ft = .3048 meters; 1 liter = 1.057 quarts and 1 quart = 1.006 liters. See NBS Monograph No. 14.

** U.S. of Weights and Measures, Price \$2.75, SD Catalog No. C-13, 1966.

TABLE OF CONTENTS

	Page
INTRODUCTION	1
Background	1
Objectives	2
DISCUSSION	2
Test Bed Helicopter	2
Weather (Ground Mapping) Radar	2
X-Band Radar Transponder	4
Passive Radar Reflectors	8
General Test Procedure	10
TEST RESULTS	12
Passive Enhancement (Reflectors)	12
Active Enhancement (Radar Transponder)	15
CONCLUSIONS	17



LIST OF ILLUSTRATIONS

Figure		Page
1	CH-53A Test Bed Helicopter (N-39)	18
2	RDR-1400 Multimode Radar System	19
3	RDR-1400 Display Control Unit	20
4	Comparison of Triangular-Corner Reflector and Square Corner Reflector	21
5	Triangular Corner Reflector	22
6	Square Corner Reflector	23
7	Summary of Passive Reflector Characteristics	24
8	Airborne Radar Approach Test Sites	25
9	Brandywine Shoals Lighthouse, Offshore Test Site	26
10	Bayside, New Jersey, Remote Test Site	27
11	NAFEC Airport Test Site	28
12	Radar Display at Bayside Test Area	29
13	Radar Display at NAFEC Test Area	30
14	Radar Display at Brandywine Shoals Lighthouse	31
15	Comparison of Vertical and Horizontal Radar Targets	32
16	Radar Display at Bayside Test Area, Single Radar Beacon	33
17	Radar Display Showing Multiple Beacon Returns Due to Sidelobe Triggering - High Radar Display Gain Setting	34
18	Radar Display at NAFEC Test Area, Single Radar Beacon	35
19	Radar Display at Brandywine Shoals Lighthouse, Radar Beacon on Lighthouse	36
20	Digital Display Unit	37

LIST OF TABLES

Table		Page
1	CH-53A Characteristics and Performance Parameters	3
2	Bendix RDR-1400 Performance Characteristics	5
3	Motorola SST-181X X-Band Transponder General Performance Characteristics	6
4	Motorola SST-181X X-Band Transponder Characteristic Verification Test Results	7

INTRODUCTION

BACKGROUND.

As the United States (U.S.) civil helicopter fleet is growing at the rate of 12 percent per year and currently encompasses over 6,000 helicopters, there is an ever-growing pressure on the Federal Aviation Administration (FAA) from helicopter operators for regulatory changes which will allow exploitation of the helicopter's unique capabilities and provide for increased vehicle productivity, expanded service, and a safer flight environment. In response, the FAA has issued a 5-year Helicopter Operations Development Plan (FAA-RD-78-101) which details programs and activities aimed at resolving the problems which are currently recognized and identifies areas of future interest. Such problems include the air traffic control (ATC) application of fixed-wing criteria and procedures to helicopters, which only serves to constrain both the helicopter and conventional traffic flow. Also recognized are the need for long-term improvements which entail upgrading the National Airspace System (NAS) to enable helicopters to employ their unique capabilities to the maximum practical extent. Specifically, the Helicopter Operations Development Plan lists five areas of helicopter operation which warrant intensive analysis and development:

Navigation/Landing,
Communications,
ATC Procedures,
Weather/Icing, and
Instrument Flight Rules (IFR) Certification.

Addressing the first of these problem areas, the optimum helicopter navigation and landing systems are not limited by line-of-sight and point reference restrictions, and must be usable at low altitudes as far as 300 nautical miles (nmi) offshore. With these constraints in mind, the airborne weather/ground mapping radar presents itself as a possible candidate for identification of offshore and remote landing sites, as an en route navigation system, as a means of providing obstacle clearance, and as a nonprecision approach aid.

Airborne weather radars have been in use by civil aviation for approximately 30 years. These radars have generally been C-band (5,000 megahertz (MHz)) with fairly large (approximately 30-inch) dish antennas and rather bulky transmitter and servo assemblies. Recently, a new generation of smaller, light-weight digital radars operating an X-band (9,000 MHz) with smaller (approximately 12-inch), flat dish antennas have become available for civil fixed-wing and helicopter use. These radars are multimode; they can be operated in a weather-avoidance mode, a ground-mapping mode, and a transponder beacon mode, which further broadens their usefulness. The application of airborne weather radars as an approach and landing aid has become known throughout the offshore support helicopter industry as an Airborne Radar Approach (ARA).

OBJECTIVES.

These Flight tests were run with a dual objective: to develop a statistical data base on ARA performance and operational procedures, and at the same time, to gain a subjective insight for the problems encountered and efforts necessary to overcome them. An additional purpose was to provide specific inputs to RTCA SC-133 to develop minimum operational standards (MOPS) for helicopter ARA use.

The statistics from the data base will be used by the FAA to develop and certify a set of standard ARA procedures. At the present time, individual offshore helicopter operators are being granted ARA certification on a case-by-case basis because no overall certification standard exists.

This report deals mainly with the more subjective aspects of the flight test; no statistically reduced data will be presented, but rather a description of the systems used and procedures which evolved with the resulting insights and conclusions will be presented. Statistical data have been developed and are presented in a comprehensive report, FAA-RD-79-99, prepared by Champlain Technology Industries.

DISCUSSION

TEST BED HELICOPTER.

N-39, the test bed helicopter, is a Sikorsky CH-53A, serial number 65026. It is a military machine on bailment to the National Aeronautics and Space Administration (NASA) from the Marine Corps. NASA had uprated the twin turbines, installed an airline-type interior, and loaned the helicopter to the FAA in support of the instrument flight rules (IFR) Helicopter Program at the National Aviation Facilities Experimental Center (NAFEC). A labeled illustration of N-39 appears in figure 1; a tabular list of performance parameters appears in table 1.

WEATHER (GROUND MAPPING) RADAR.

N-39 is equipped with a Bendix RDR-1400 multimode X-band radar which consists of three physically separate units: an indicator/control unit, a receiver/transmitter, and a pitch and roll stabilized radar antenna (see figure 2). Figure 3 illustrates the indicator/control unit and a typical weather return depiction. The RDR-1400 can be operated in any of six modes: three search modes (SRCH), two weather modes (WX), and a beacon-only mode (BCN). The three search modes are normally used in the ranges of up to 20 nmi and can detect primary surface target returns down to a minimum range of 600 yards. Search 1 has clutter rejection circuitry, at a sacrifice in sensitivity, and is intended for short-range (i.e., 2.5, 5, 10, and 20 nmi) mapping of targets in a sea-clutter environment. Search 2 is similar to Search 1 but with the absence of clutter rejection and with a consequent increase in sensitivity. Search 3 uses a longer pulse to put more energy into the target and thus

TABLE 1. CH-53A CHARACTERISTICS AND PERFORMANCE PARAMETERS

<u>Characteristic</u>	<u>Metric</u>	<u>English</u>
Empty weight	11575.0 kg	25525.0 lb
Normal takeoff weight	16330.0 kg	36000.0 lb
Maximum gross weight	31704.0 kg	69750.0 lb
Main rotor blades		
radius	11.0 m	36.0 ft
chord	0.7 m	2.16 ft
number	6	6
Tail rotor blades		
radius	2.4 m	8.0 ft
chord	0.4 m	1.28 ft
number	4	4
Main shaft forward tilt	5°	5°
Disc loading	394.0 N/m ²	8.23 lb/ft ²
Number of engines	2	2
Engine power (each)	2.95x10 ² watts	39.50x10 ² hp
Maximum cruise speed	315.15 km/hr	170.0 knots
Normal cruise speed	241.0 km/hr	130.0 knots
Maximum endurance	2 hours	2 hours
Crew	3	3

maximize clutter returns, thereby outlining such nonclutter targets as oil slicks. The two weather avoidance modes furnish weather information relative to rain cloud formation, rainfall rate, thunderstorm areas, and areas of possible icing. High-density rainfall returns are contoured into dark areas on the display, and the second weather mode WXA or "Weather Alert" alternately displays high-density rainfall as contour and noncontour at a 1.25-Hz rate as an attention-getting device.

In the beacon-only mode, the radar transmits on the normal interrogation frequency of 9375 MHz which is received by a transponder beacon. The beacon then replies on the special beacon frequency of 9310 MHz which is received by the radar. The radar indicator displays the range and bearing to the beacon, free of ground or other primary radar returns.

Before commencement of flight testing, a Bendix field engineer inspected the installation of the RDR-1400 in N-39 and its operation, both on the ground and in flight, and determined that both were satisfactory. A list of RDR-1400 performance characteristics, as installed in N-39, appears in table 2.

X-BAND RADAR TRANSPONDER (BEACON).

A radar transponder (or radar beacon as it is usually called) is essentially a radar receiver combined with a radar transmitter operating on different frequencies. When the beacon receiver detects a pulse interrogation (radar transmission) on the frequency to which it is tuned (9375 MHz in our case), it triggers the beacon transmitter to reply with a pulse or series of pulses on its reply frequency (9310 MHz in our case). This beacon reply is received at the interrogating radar by a special receiver as a signal return of much greater strength than a primary return from the same radar range.

The beacon used for these tests were Motorola SST-181X general purpose X-band transponders, which were obtained from U.S. Air Force material stock. Table 3 lists a summary of SST-181X parameters.

Upon receipt at NAFEC, the beacons underwent characteristic verification tests; a tabular summary of these test results appears in table 4. For the flight tests, the beacons were used at the NAFEC airport, at a remote site (Bayside, New Jersey), and at an offshore site (Brandywine Lighthouse in Delaware Bay). The beacons were fitted into a waterproof case and portable power was furnished by two 12-volt marine storage batteries connected in series. The entire package was self-contained and portable enough to be transported to the test site, set up, and made operational prior to each flight. The lighthouse beacon was connected to the lighthouse power as a power supply was built into the water-proof case and was left to run continuously through the test period.

TABLE 2. BENDIX RDR-1400 PERFORMANCE CHARACTERISTICS

<u>Characteristics</u>	<u>Description</u>
Power requirement	28 V d.c., 4.2 A; 115 V a.c., 400 Hz, 3 A
RF power output	10-kW peak
Frequency	Search, weather modes: transmit and receive 9375-MHz beacon mode: trans- mit 9375 MHz; receive 9310 MHz
Pulse width	Search 1, Search 2: 20 nmi range: 0.5 μ s; 20-nmi range 2.3 μ s; Search 3, WX, WXA, BCN: 2.35 μ s
Scan angle	120° ($\pm 60^\circ$), 40° ($\pm 20^\circ$)
Scan rate	24°/sec
Data rate (update rate)	5 sec/update ($\pm 60^\circ$), 2 sec/update ($\pm 20^\circ$) target centered
Pulse repetition frequency	200 Hz 20-nmi range; 800 Hz 20-nmi range
Sensitivity time control (STC)	40 nmi (using 12-inch antenna) (64 km)
Minimum range	600 yards (549 m)
Maximum weather range	240 nmi (386 km)
Antenna size, gain	Planar 12-inch (30 cm) phased array, 28.2 dB
Elevation angle	Manual tilt $\pm 15^\circ$
Stabilization range	Vector sum (pitch, roll, tilt) of 30°
Display size	4.34 inches x 3.33 inches (11 cm x 8.5 cm) rectangular CRT
Indicator size	6.25 inches x 6.25 inches (16 cm x 16 cm) see figures 3 and 4
Antenna beamwidth	Azimuth: approximately 7.5°. Eleva- tion: undefined

TABLE 3. MOTOROLA SST-181X X-BAND TRANSPONDER GENERAL PERFORMANCE CHARACTERISTICS

<u>Characteristic</u>	<u>Description</u>
Primary power	24-30 V d.c., 0.55 A (stdby), 0.7 A (1,000 pps)
Recovery time	50 μ s Max.
Delay time	1 μ s nominal; adjustable to 4.3 μ s Max.
Dimensions	(3.36 x 2.90 x 3.96) in; (8.53 x 7.37 x 10.06) cm
Weight	3.3 lb; 1.5 kg
Receiver frequency	9375 MHz
Receiver bandwidth	18 MHz
Receiver sensitivity	-68 dBm nominal
Receiver pulse width	0.25 to 5.0 μ s
Transmitter frequency	9310 MHz
Transmitter pulse width	290-310 μ s
Transmitter power	400 watts (peak) nominal
Antenna gain	4 dB nominal

TABLE 4. MOTOROLA SST-181X X-BAND TRANSPONDER CHARACTERISTIC VERIFICATION TEST RESULTS

<u>Characteristic</u>	<u>Description</u>
Receiver frequency	9375 MHz
Receiver sensitivity	-66.83 dBm average
Transmitter frequency	9310 MHz
Transmitter pulse width	298.33 μ s average
Transmitter power	507.4 watts peak average

PASSIVE RADAR REFLECTORS.

Target enhancement obtained through the use of passive radar reflectors, such as corner reflectors and box reflectors, was evaluated as an ARA aid early in the flight test program. Reflectors of this type are constructed of three mutually orthogonal planar surfaces which intersect at a point thus forming a "corner." The corner reflector takes advantage of large radar cross-sections obtained from this set of three properly oriented flat plates by returning radiation over a much wider range of incident angles than would a single flat plate of the same cross-sectional area. Two corner reflectors, a triangular and a square, or box corner, are shown in figure 4. The incident radiation which is sequentially reflected from all three of the planes will be sent back in the direction it came from.

The maximum amount of energy will be returned to the radar if its radiation is directed into the corner reflector in such a way that the incident radiation vector makes equal angles with all three planes. This is generally referred to as the optimum return configuration. As the direction of incident radiation is changed with respect to the optimum position, the amount of returned energy diminishes with the radar cross-section, but does so rather slowly when compared to the energy reflected by a single flat plate at optimum orientation.

As can be seen from inspecting figure 4, the square corner reflector will, under optimum conditions, present a radar cross-section equal to nine times that of the triangular corner reflector. There is only twice as much material or surface area in the square corner reflector, but it is used more effectively. This may seem somewhat unlikely upon initial inspection of figure 4, but may be demonstrated by the following geometric exercise which is pictorially represented in figures 5 and 6. Figure 5 represents a triangular trihedral corner of length a , and figure 6 is a square trihedral corner of the same interior dimension. For this example, only incident rays which are reflected from each of the three planes, and only those rays which are perpendicular to the plane ABC, are considered. Triple reflection at incident angles, other than optimum, and trihedral or double reflection with reflected energy paralleled to the incident beam, are common but would only serve to complicate this example. Considering the triangular reflector, figure 5, the path of a typical triply reflected ray is shown by lines 1, 2, and 3. The ray has entered, and also leaves, the reflector along a line perpendicular to the plane of the paper. Points 1 and 3 represent the initial and final points of reflection, respectively, where point 2 is the intermediate point.

Some interesting conclusions can be drawn upon inspection of ray paths 1, 2, and 3. First, points 1 and 3 form a line which, when projected upon the plane of the paper, goes through O, each point being equidistant from O. Second, line 12 is parallel to line OB, and line 23 is parallel to line OC. Thus, 12 and 23 are parallel to the normals of the initial plane AOC and final plane AOB, respectively. Therefore, the incident ray at point 1 will be directed parallel to the projection of the normal of the incident plane AOC toward point 2, which is the image of point 1 on plane BOC. Similarly, the ray at point 2 is reflected parallel to the normal of the final plane AOB toward

point 3, which is the image of point 2 on plane AOB. Also, the incident and final points must be equidistant from the projection of the intersection of all three planes, point 0, and all three points on the projection must form a straight line. Incident rays which do not meet these criteria will not be reflected in the direction of the source. An example is the incident ray striking point 4 on plane AOC in figure 5. It is reflected to point 5 in plane BOC but will not be reflected at point 6, since plane AOB does not extend that far (it does, however, when considering the square corner reflector of the same dimension, as shown in figure 6). Therefore, the external corners of the triangular corner reflector do not participate in triple reflection, and their area is lost in terms of effective area.

The term "effective area" refers to that portion of the projected cross-section of a corner reflector which participates in the return of incident radiation to its source. It is also referred to as "equivalent flat plate area." A method of determining this effective area, using the criteria just established, is shown by the following procedure: rotate each plane in the direction of its normal, about the intersection point 0, until its exterior edge is again in the plane formed by the exterior edges. This is now the image of the plane projected through point 0. Plane AOB would rotate about 0 to form image plane DOE; AOC and BOC would image to planes EOF and EOF, respectively. For the triangular corner reflector, the area common to both the projection of the actual reflector, ABC, and that of its image through 0, DEF, is equal to the effective area, which is a regular hexagon of side length $\sqrt{2}/3$ a, GHIJKL.

For the square corner reflector, it can be shown by using the method outlined above that the projection of the actual reflector and its image through 0 are identical; i.e., any ray which falls on the projection and is perpendicular to the plane of the projection cannot fail to be triply reflected. Therefore, the effective area of the square-corner reflector is the same as the area of the projection ABCDEF, which is a regular hexagon of side length a, the same length as the corner length. A mathematical derivation of the effective areas of both reflectors appears in their respective figures. Also, the radar cross-section is inversely proportional to the square of the radar wavelength. Thus, it is apparent that small corner reflectors, in order to be useful targets, must be used in conjunction with higher frequency radars.

Two additional types of passive reflectors are considered here. The first, a flat plate reflector, is mentioned not because of its usefulness, but because it is the standard against which other passive reflectors are measured. Obviously, for a flat plate to return a maximum of the incident radar beam, it must be oriented so that angles θ and ϕ , as shown in figure 7, equal zero degrees. The level of returned energy falls off rapidly with increasing values of these angles, making the practical value of this type of reflector very low. The second type of reflector, which was not used in the flight test but is of interest because of its wide angular response, is the 180° cap Luneburg lens (figure 7). The Luneburg lens consists of a dielectric sphere and a reflective cap which form a lens having the property of collecting the incident energy which falls on the uncapped surface, or hemisphere, refracting it through the sphere, and bringing it to a focus at the center of the surface of the opposite hemisphere. If a reflective surface is placed at

this point, the energy will be reradiated in the direction from which it originated. As the direction of the incident radiation is changed, the focal point shifts accordingly, and the target will respond over a large range of incident angles.

A comparison of the characteristics of the most widely used types of passive reflectors is shown in figure 7. Inspection of this figure shows that for a given dimension, "a" in this case, and optimum geometry or incident energy coinciding with the axis of symmetry, the Luneburg lens is the most efficient reradiator followed by the square corner, triangular corner, and flat plate.

Thus, it would seem that most passive reflectors would be of the Luneburg lens and square-corner types because of their reradiating efficiency. However, in selecting a reradiator for actual use, there are often practical considerations which can outweigh theoretical values. The first and most important consideration is cost. It is somewhat surprising to discover that all the described passive reflectors, save the flat plate, would, when precisely constructed to a usefully large dimension ($a \leq 1.5m$), cost more and provide less azimuthal coverage than the transponder beacon described previously. The second consideration is the effort and length of time that must be expended in the construction of the reflector. Precision in construction and bracing to achieve durability is a necessity and accounts for the high cost. It is also a liability in field use in that the reinforced structure results in a heavy and awkward unit. Another liability is that dents or misalignment of planes or similar damage, which may be incurred in normal field use, result not only in reduced strength of reflection by misdirecting the radiation, but may also cause out-of-phase reflection and subsequent cancellation, or nulls, severely limiting the usefulness of the unit.

GENERAL TEST PROCEDURE.

This effort was undertaken in order to gather a data base on the ARA using simulated IFR approach techniques at offshore, airport, and remote land site environments. Target enhancement and definition was provided through the use of the previously described active transponder beacons and passive corner reflectors.

The three sites chosen were the NAFEC/Atlantic City Airport for the airport approaches, Brandywine Lighthouse for the offshore approaches, and the small fishing village of Bayside, New Jersey, for the remote site approaches. A simplified map showing the location of each site is presented as figure 8. As can be seen from inspection of figure 8, the three sites form a rough isosceles triangle whose circumference of 104 nmi (193 km) allowed a round-robin type of data flight with multiple approaches at each location.

A picture of the Brandywine Shoals Lighthouse with the beacon location detailed is shown in figure 9. The top of the light chamber is approximately 70 feet (21 m) above mean sea level (m.s.l.) with the beacon location about 48 feet (15 m) above m.s.l. As can be seen, the lighthouse itself presents a rather large radar target (approximate calculated X-band radar cross-section:

$100,000 \text{ m}^2$ not including the surrounding breakwater) against a low-clutter background. Passive enhancement by corner reflectors was regarded as unnecessary, and this proved true as the lighthouse was almost always displayed as a prominent target by the RDR-1400 from ranges of beyond 20 nmi at an altitude of 1,000 feet m.s.l.

Figure 10 shows the remote site, Bayside, New Jersey, as viewed from the approaching test bed helicopter. The beacon and corner reflector locations are indicated. The corner reflector is a large square corner oriented so as to provide a maximum return when approaching along a direct line from NAFEC; the beacon coverage is omnidirectional and requires no special orientation. The tidal estuary (name unknown) has the shape of a large question mark, and it was hoped that it would be a geographical landmark which would show up well on the radar, thus providing additional aid for site identification in the primary return mode.

A map of the NAFEC airfield, the airport site, is shown as figure 11. The beacon sites are labeled as are the positions of the corner reflectors. The airport area is comprised of more than 5,000 acres of predominantly cleared land surrounded by relatively flat scrub pine and oak woodland. Several hangers and related support structures are positioned on the various ramp areas as shown.

Due to the availability of several small (25.5-inch, 65-cm) corner reflectors, the first set of test flights were based on primary radar return information with corner reflectors put to use at the remote and airport sites. These corner reflectors were manufactured by a contractor for use in a ground control approach (GCA) system which had been installed at NAFEC but was no longer in operation. They are of a rigidly braced alloy construction and are built to precise tolerances. Each reflector presents a maximum radar cross-section of 715 m^2 to the RDR-1400A. During the course of the investigation, it was decided to use a larger corner reflector to realize an improvement in signal return. These larger reflectors had a corner dimension of 68-inches (73-cm) and presented a maximum radar cross-section of $36,153 \text{ m}^2$ to the RDR-1400A. The larger reflectors were built in the project laboratory of 1/8-inch (0.32-cm) sheet aluminum and angle iron which, unfortunately, did not lend itself to the fabrication of a very rigid or precisely aligned product.

During the primary-return (passive) tests, a total of 25 approaches were made to all three sites: 13 at the airport site, 7 at the remote site, and 5 at the offshore site.

Upon obtaining the transponder beacons, test emphasis shifted to using the beacons to provide active target enhancement. During this phase of the test program, a total of 35 single-beacon approaches were made to all three sites, 13 each at the airport and remote sites, and 9 at the offshore site.

At the conclusion of the single-beacon tests, several flights were undertaken with two beacons defining the desired runway. One beacon was placed to define the approach threshold, while another was placed at midrunway, the stop end,

and beyond the stop end of the runway on centerline. The idea here was to give some lateral, or cross-track guidance, by allowing a reference of centerline to be established by ascertaining the azimuth angle of the line between the centroid of the two beacon returns. This would be of great value in establishing a desired track and wind correction angle.

TEST RESULTS

PASSIVE ENHANCEMENT (REFLECTORS).

For these tests, a single small reflector was initially placed at the remote site, multiple reflectors were used at the airport site, and no enhancement was used at the offshore site. For the majority of the flights within this test, the single small reflector at the remote site was replaced by a single large reflector in the hope of allowing a positive identification of the site.

REMOTE SITE. The reflector at the remote site was oriented to provide a maximum return when approaching from the direction of NAFEC, as this allowed the NAFEC remote site leg of the flight to terminate in long straight-in approach to Bayside.

The coastline of New Jersey along Delaware Bay was always very discernable on the RDR-1400A. Large geographical features of this type such as bays, large river mouths, islands, etc., make good radar landmarks. It was recognized that discerning more precise targets amongst these features could prove difficult, so it was decided to place a corner reflector near Bayside to further enhance the effect of the unique coastline geography by the "bright spot" of the reflector return. However, as figure 12 shows, the radar return of the Bayside area, as seen from the approaching helicopter at approximately 4-nmi (6.4 km) range and 500-foot (152 m) altitude, is not well enough defined to be a positive identification. The strong return at 3.5 nmi (5.6 km) and dead ahead is from the buildings, boats, and large corner reflector at Bayside proper, while the two weaker returns just beyond are the islands on the far side of the tidal estuary. The large return at 50° off of aircraft heading and 2-nmi range is an anchorage for pleasure boats on the Cohansey River near Greenwich, New Jersey. Numerous small craft were at anchor making good radar targets. The distinctive shape of the tidal estuary is not visible in this photo, as the gain control has been adjusted so as to allow display of only the strongest returns. If the gain were adjusted to allow display of the weaker returns and, therefore, show a "map" of the coastline, the desired target of Bayside would be obscured by the consequent ground clutter.

As an additional experiment, the large corner reflector was placed face down on alternating approaches. No change in the apparent appearance or brightness of the Bayside target was noticeable in the absence of the reflector. It should be noted here that the grassy marshland that surrounds Bayside is thought by many authorities to present a background or clutter target of approximately $8,000 \text{ m}^2$ for this type of radar. The calculated maximum radar

cross-section of the large corner reflector is $36,153 \text{ m}^2$ and should have shown up well against this type of background. That it did not can probably be explained by the previously mentioned lack of rigidity and precision in construction.

Upon further investigation of corner reflector theory, we find that the larger the reflector, the more care must be exercised in construction or the unit will be subject to misaligned returns and destructive interference which can drastically reduce the radar cross-section. That was probably the case here since the reflector return, when identified, changed in intensity very sharply as a function of aspect angle. Even when the helicopter was hovered at a range of 1-nmi and 500-foot attitude and the reflector target return was positively identified, the return intensity was observed to vary greatly with the small altitude changes necessary to keep the aircraft at hover.

The original small corner reflector used at Bayside was completely invisible amid the background clutter at all times. These smaller reflectors were precisely constructed and rigidly braced, but were of a size which presented a maximum cross-section of only 715 m^2 and were probably lost in the ground clutter. Therefore, from these and similar results, passive reflector enhancement, as applied to this remote site of Bayside, New Jersey, was not sufficient to give a radar return which was discernible from ground clutter.

AIRPORT SITE. Reflectors at NAFEC, the airport site, were oriented as shown in figure 11, with the threshold or central reflector being a large corner ($36,153 \text{ m}^2$) and the other two reflectors being the smaller corner (715 m^2). Figure 13 is a photo of the radar display during an approach from due north with the reflectors as shown. This particular siting was chosen because runway 17/35 is a closed runway, and the multiple slow helicopter approaches would not interfere with active runway traffic. A large cleared area is adjacent to the threshold of 17 which allowed convenient placement and movement of the reflectors.

Regarding figure 13, the desired target on the runway threshold is at a range and azimuth of approximately 3 nmi and 5° right of the aircraft heading. As can be seen from the photograph, several small or weak targets appear in this region but are impossible to use for positive identification purposes. Also, no triangular pattern appears in this picture; indeed the pattern never appeared on the radar display for a variety of reasons. First, the low brushy second-growth type of flat terrain surrounding NAFEC presents a clutter target size of $10,000 \text{ m}^2$ to this type of radar, in the search 1 or search 2 mode, as it was being operated here. Therefore, the smaller reflectors would have been invisible amid the ground clutter no matter what gain setting was used. Secondly, the radar beam width of 7.5° would have completely covered the dual target at the range of 3-nmi (which would be separated by 7.5°) and the smaller two reflectors would show up, not as two distinct targets, but as one spread target of approximately 15° .

Returning to figure 13, the large return at 4 nmi and aircraft heading is a composite of the return from the large hangar on the NAFEC ramp and the aircraft parked on the ramp in front of the hangar. The return at 3.5 nmi and approximately 50° right of the aircraft heading is from the corrugated metal hangars used by the New Jersey Air National Guard in their alert area. The large number of strong returns in the 1- to 2-nmi range is ground clutter which has been brought to prominence by the approximate 4° tilt down setting used when this picture was taken. However, as figure 13 shows, the results from these tests were inconclusive at best, and at no time could a positive identification of the desired landing site be made by radar alone.

OFFSHORE SITE. No passive enhancement was used at the offshore site, Brandywine Shoals Lighthouse, as it presented a very large calculated radar cross-section of 100,000 m² against a low-clutter background. No difficulties were encountered in getting a return from the lighthouse or distinguishing it from sea clutter, even at ranges in excess of 20 nmi at altitudes of 1,000 feet m.s.l. Prominent though the lighthouse target seemed, it was, at times virtually indistinguishable from the targets presented by nearby slow-moving shipping traffic, and was often not positively identifiable until visual contact was established. This would be a very close approximation of the conditions presented to a pilot servicing an offshore oil rig which is one of a group or "cluster" of six to eight rigs within a circular area of 1 nmi radius, a not unusual case on the Gulf of Mexico.

Another complicating factor is provided by the 7.5° beam width of the RDR-1400; when two or more targets are within one beam width of each other, as viewed from the radar antenna, they appear as one elongated return of 7.5° plus the actual angular separation as seen from the radar antenna. That is to say that a cluster of rigs, each rig separated by a 0.5 nmi, 2 nmi in breadth, would look like one composite target from the maximum target acquisition range down to a range of 3.8 nmi from the cluster. Only within 3.8 nmi would the individual targets, or rigs, start to be resolved into separate returns on the radar display. Also, one would think that the physical size or at least the azimuthal size of the target would bear a direct relationship to the size of the displayed return, but the radar beam width has a tendency to mask this and cause all "discrete" returns, such as various sized ships at the same range to be displayed as targets of similar size.

Figure 14 shows a photograph of the radar display during an approach to the Brandywine Lighthouse from the direction of Bayside, New Jersey. The lighthouse appears as the target at a range of 3 nmi and slightly to the right of aircraft heading. Notice several additional targets within a 2-nmi radius of the lighthouse; these are various types and sizes of ships both at anchor and underway and present targets that are very similar to the target displayed by the lighthouse itself. Therefore, while the lighthouse was a reliable target in terms of return strength, positive identification was difficult because of the large number of nearby ships and other craft that also present strong targets. Also, at times a ship would pass within 0.25 nmi (400 m) of the lighthouse and present a composite return in conjunction with the lighthouse. When the two separated, identification was very difficult even though the lighthouse

presented a "vertical" target while the ships presented a "horizontal" or azimuthal target. This can be shown in the diagram of figure 15 depicting two rectangular flat-plate targets of dimension 10 m x 100 m which are illuminated by a radar beam such as generated by the RDR-1400. In case A, the target is oriented so that the 100-m side is in the azimuthal direction. In case B, the target is rotated 90° so that the 10-m length is now lying in the azimuthal sweep.

If both targets were reviewed from the same range, say 5 nmi (9.3 km), each target would be displayed as a return of essentially the same size (8.12° for A vs. 7.56° for B) since the beam width is much larger than the azimuthal size of each target as viewed from the radar: 0.62° for A vs. 0.06° for B. This effect is enhanced with increasing range as the physical azimuth subtended by each target will asymptotically approach zero, while the return size will similarly approach 7.5° for each. Likewise, as the range decreases, the physical azimuth will increase exponentially allowing a more realistic display of the relative target sizes. This limitation imposed by the 7.5° beam width is difficult to overcome without extensive design changes in the radar itself. Such changes to narrow the beam width would be likely to have a detrimental effect on the size, weight, and cost of the radar set and could detract from its primary purpose of weather detection.

RESULTS. The results of the passive enhancement and primary return testing are inconclusive including the offshore or lighthouse case where target acquisition was not a factor but target identification was. Passive enhancement of desired targets is attractive because no source of power is required, and unless catastrophically damaged in some way, the reflector remains a permanent maintenance-free device. Several drawbacks present themselves, however. First is that in order to be effective in landside airport and remote operations, the maximum cross-section presented by the reflector must be much larger than the surrounding ground clutter. This implies a large unwieldy object which would be difficult to install, subject to wind loading, and could conceivably become an obstruction itself. Second, none of the reflectors described in this report, except the Luneburgh lens, offer 180° coverage in azimuth; if a greater azimuth coverage is required, multiple reflectors have to be installed, further compounding the problems. Third, as mentioned previously, a large precisely constructed reflector is a very expensive item; much more so than the solid state, active radar transponders, or beacons available at the present time.

In summary of these remote passive enhancement tests, one can say that if one knows precisely what one is looking at on the radar screen, one can make an educated guess as to which return is the desired. Without this fore-knowledge, positive identification of the landing site by passive radar return alone is impossible.

ACTIVE ENHANCEMENT (RADAR TRANSPONDER).

For these tests, single beacons of the type described earlier in this report were placed at the remote site, airport site, and the offshore site. The same type of round-robin flights were conducted as in the passive enhancement flights.

REMOTE SITE. Figure 16 shows the radar display during the initial phase of a single-beacon airborne radar approach to the remote site, Bayside, New Jersey, as shown in figure 10. This is a typical representation of a beacon target at a fairly long range. The gain control is at maximum and the tilt control is set at -2° . The tilt adjustment was especially critical as range decreased and declination angle to the target approached the magnitude of the radar beam width (undefined by Bendix but assumed to be comparable to the azimuth beam width of 7.5°). Under these conditions, which occurred near the end of the approach during a period of increasingly high workload for the crew members, misadjustment of the tilt or gain controls would result in losing the target for at least one scan; a critical loss, since at the slow update rate of 1/5 hertz, the target will not be refreshed for at least 5 seconds. If reduced azimuth is selected ($\pm 20^{\circ}$ vs. $\pm 60^{\circ}$), the update rate increases to 3/5 hertz, but the target may be lost if offset approach or yawing maneuvers are performed. At this point, a low-gain control setting is needed; if the gain is too high, sidelobes from the radar antenna will cause receivable returns from the beacon, causing "wrap around" or multiple beacon returns at a constant range. An example of multiple returns due to high gain setting is shown in figure 17. Under these conditions, the correct azimuth angle to the beacon becomes hard to judge correctly and a downward adjustment of the gain (as the copilot is doing in this picture) is necessary before a correct reading can be made.

An explanation of the digital display unit, shown to the left of the radar display in the beacon return pictures, appears in figure 20. This display was fabricated by NAFEC project personnel as an aid in correlating the ground-based radar tracking data with the airborne radar photographic data for statistical assessments of accuracy and flight technical error.

AIRPORT SITE. Figure 18 shows the radar display during the final stages of an approach to the airport site, NAFEC, with a beacon at ground level near the threshold of runway 26 as shown in figure 11. Notice that when the radar is in the "BCN" or beacon-only mode as shown, only beacon returns are displayed; no primary return weather, obstacles, or ground clutter are displayed. If an obstacle such as terrain, buildings, or other structures existed between the beacon and the aircraft at this point, no information as to the nature of this obstacle could be obtained from the radar display in the "BCN" mode. Several types of commercially available radars allow display of both beacon and ground-mapping information simultaneously, thus allowing positive target identification as well as obstruction clearance.

OFFSHORE SITE. Finally, figure 19 shows the beacon return from a beacon mounted on the Brandywine Shoals Lighthouse as detailed in figure 9. This photo was taken soon after departure from NAFEC at a range of approximately 28 nmi (52 km). There is no possibility here of confusing the lighthouse return with that of a passing ship as there was during the primary return tests since, as previously mentioned, the radar displays only beacon returns in this mode. However, if this were but a single oil rig in a cluster of rigs, the beacon would make identification of the desired rig an easy matter, but an approach path which would insure safe clearance of the rest of the cluster rigs would have to be determined by other means.

CONCLUSIONS

The ARA is a practical method of nonprecision approach when used in conjunction with a method of target enhancement or definition, the most practical being active enhancement. The data and subjective insights gathered during the course of this flight test program lead to the following conclusions:

1. For positive target definition and to insure a strong radar return, target enhancement is required.
 - a. Passive enhancement, while an attractive concept from the viewpoint of little or no maintenance or reliability problems, has important limitations with respect to size, construction, ease of placement, and cost of the reflectors. Passive enhancement would perhaps find optimum application in remote areas where a minimum of clutter exists.
 - b. Active enhancement is a practical method of target enhancement. It assures both target identification and a strong return signal. The problem of supplying power to the unit may prove difficult in remote areas, and the units are not maintenance free. However, these are the only drawbacks in comparison to passive reflectors, as beacons are less expensive to procure, smaller, easier to deploy, and provide a more uniform and stronger return signal than do the passive devices.
2. The 7.5° beamwidth is too broad to allow resolution of reflector or beacon patterns as an aid in recognition. Multiple targets are discernible only when separated by more than 7.5° as viewed from the radar antenna.
3. An automatic gain control (AGC) would offset the critical shortcoming of the system encountered during the final stages of the approach when return signal strength is increasing rapidly, and pilot workload is increased by the frequent gain adjustments necessary to retain target definition.
4. The slow scan rate of the airborne radar causes lags in target position update information of up to 10 seconds, depending on target azimuth and scan angle setting. Increasing the scan rate of the radar would offset a critical shortcoming of the system encountered during the final stages of the approach when small changes in aircraft heading can result in large changes in target azimuth. The slow update rate of 1/5 hertz can result in a complete loss of target during this stage of the approach.

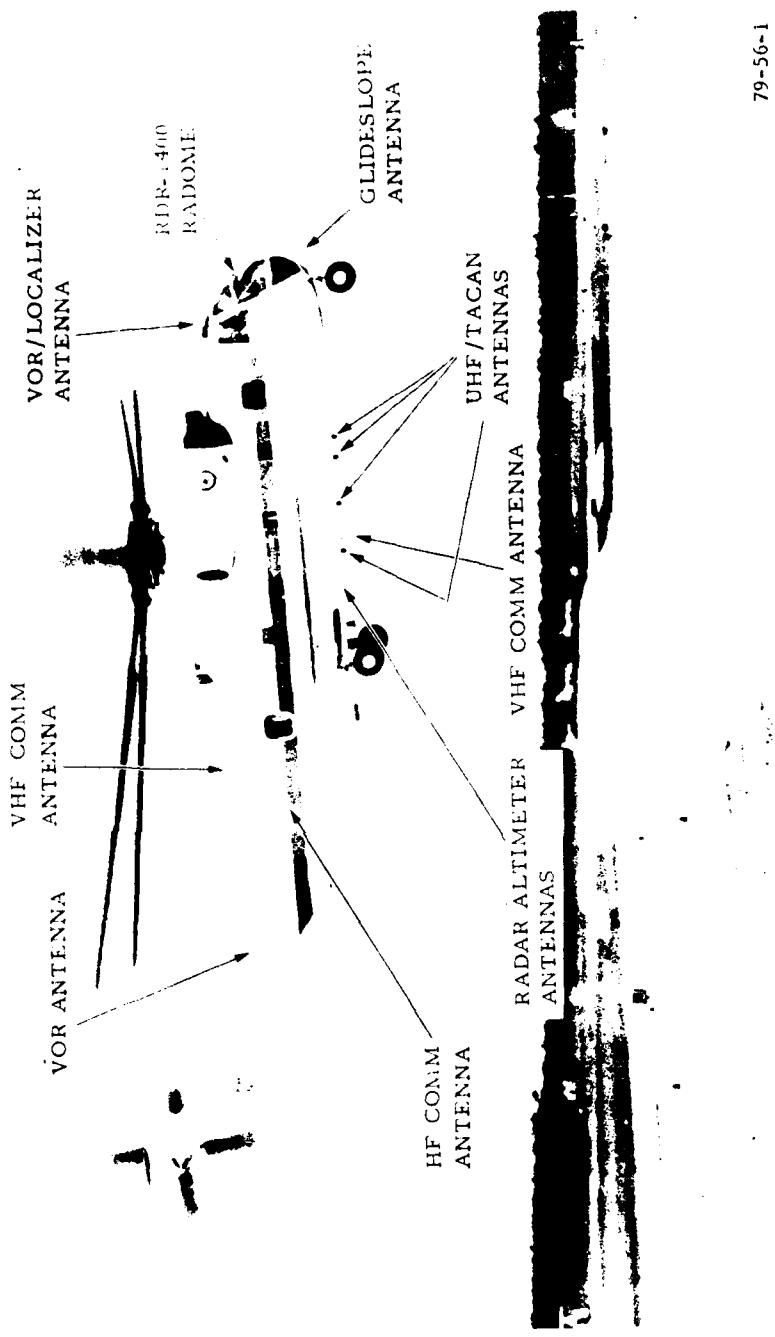
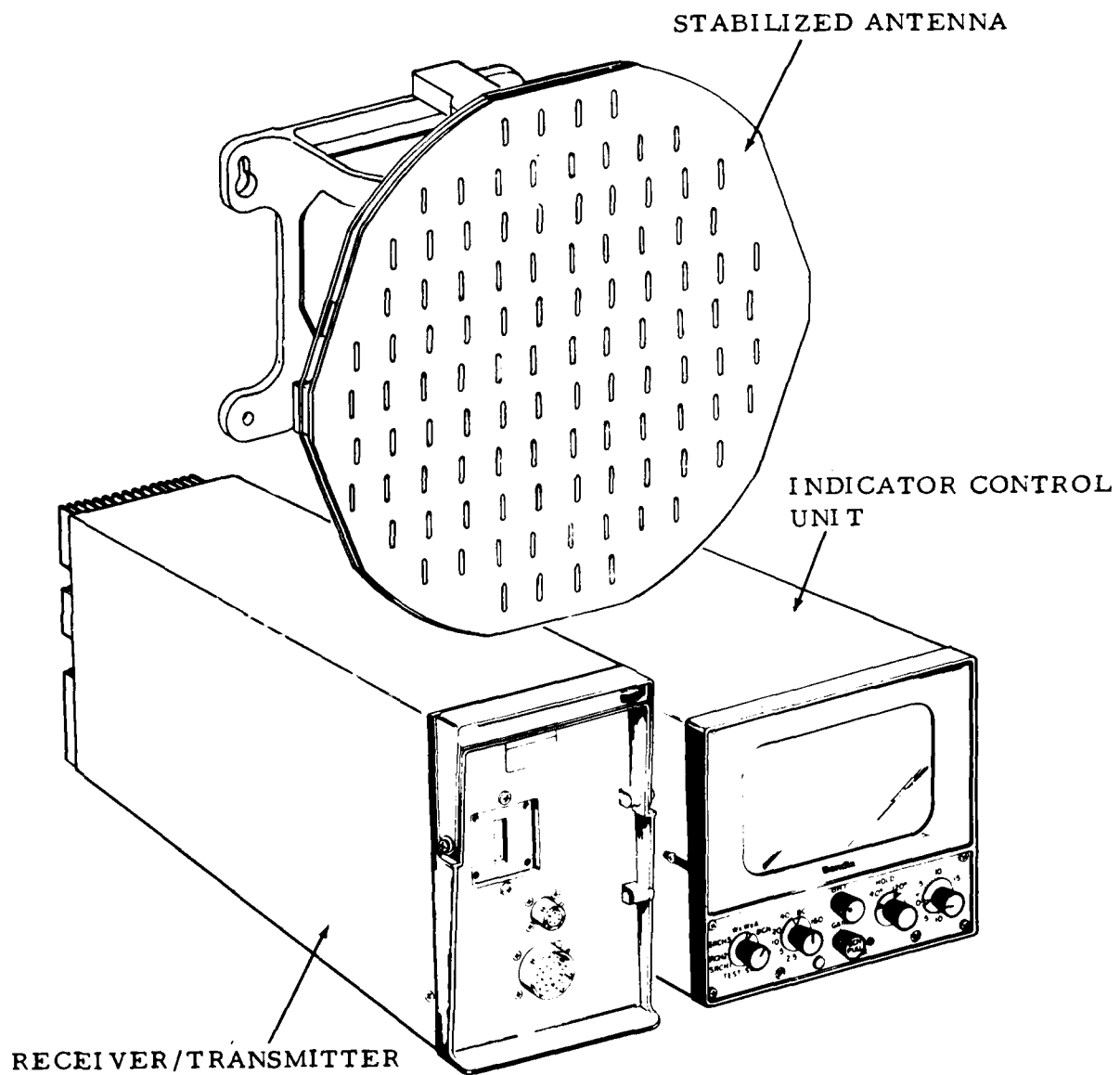


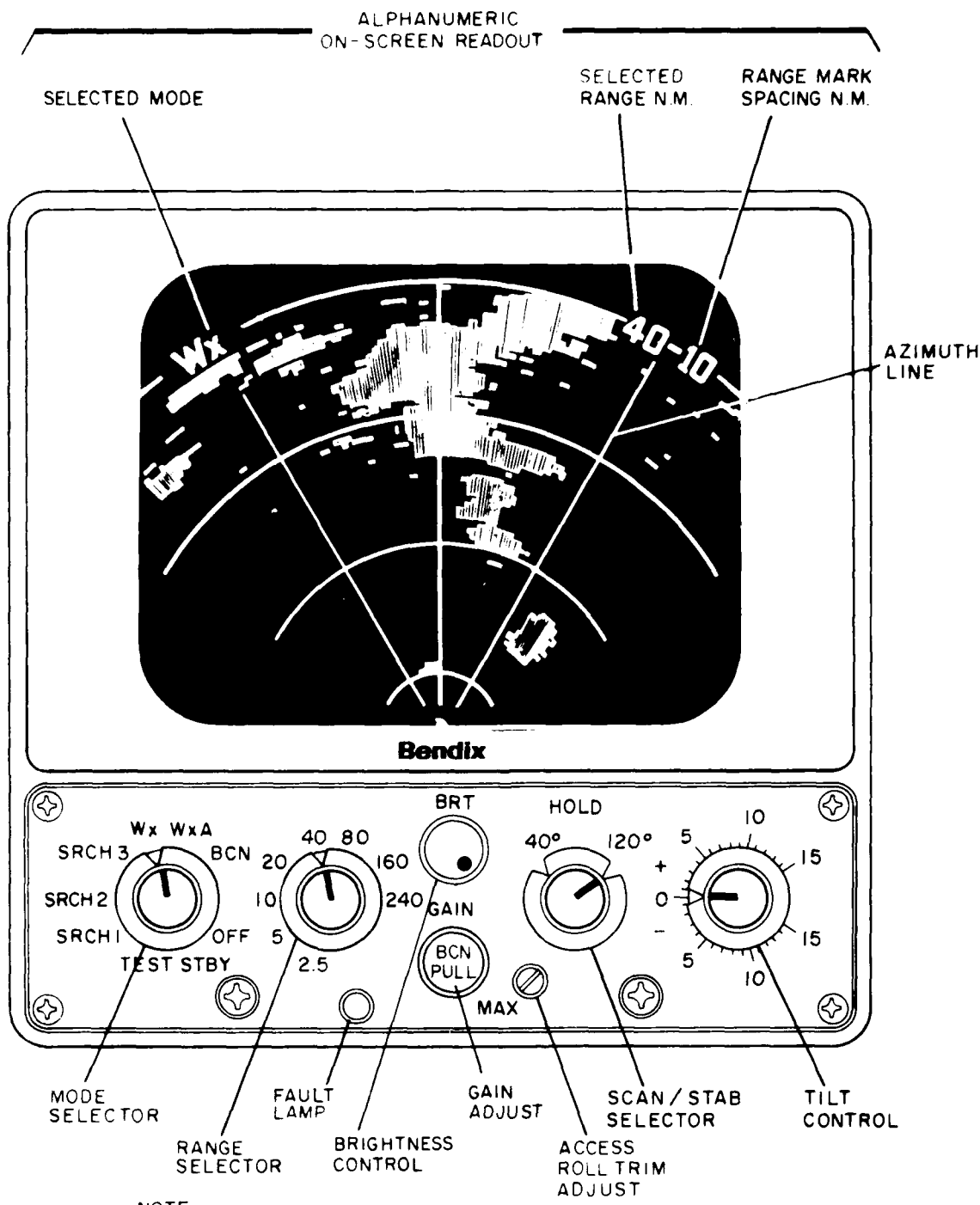
FIGURE 1. CH-53A TEST BED HELICOPTER (N-39)

79-56-1



79-56-2

FIGURE 2. RDR-1400 MULTIMODE RADAR SYSTEM



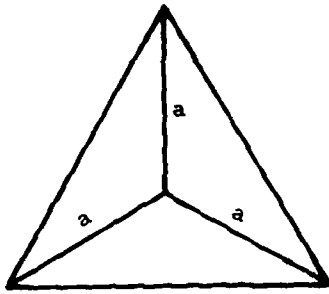
NOTE:

BCN MODE PROVIDED IN IN-1402A AND IN-1402B

79-56-3

2043038A

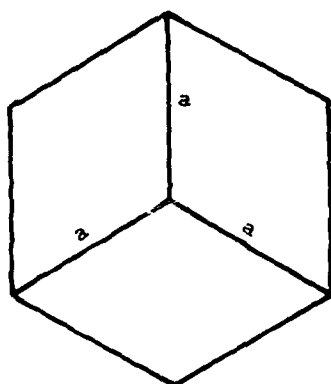
FIGURE 3. RDR-1400 DISPLAY CONTROL UNIT



MAXIMUM RADAR CROSS SECTION

$$\sigma_s = \frac{4\pi a^4}{3\lambda^2}$$

TRIANGULAR CORNER REFLECTOR



MAXIMUM RADAR CROSS SECTION

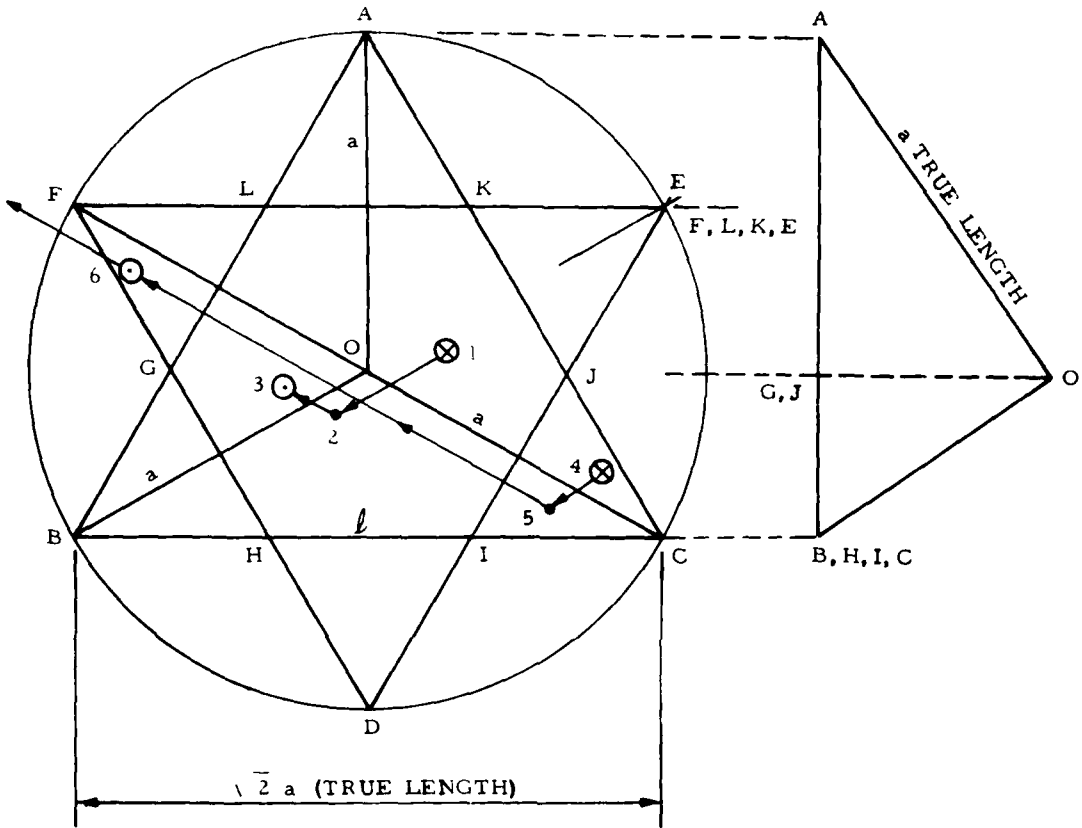
$$\sigma_s = \frac{12\pi a^4}{\lambda^2}$$

SQUARE CORNER REFLECTOR

λ = RADAR WAVELENGTH = 3.2 cm

79-56-4

FIGURE 4. COMPARISON OF TRIANGULAR-CORNER REFLECTOR AND
SQUARE CORNER REFLECTOR



$S = \text{EFFECTIVE AREA} = \text{AREA OF REGULAR HEXAGON } GHIJKL$

$S = \text{AREA OF REGULAR HEXAGON OF SIDE LENGTH } \ell = \frac{3\sqrt{3}}{2} \ell^2$

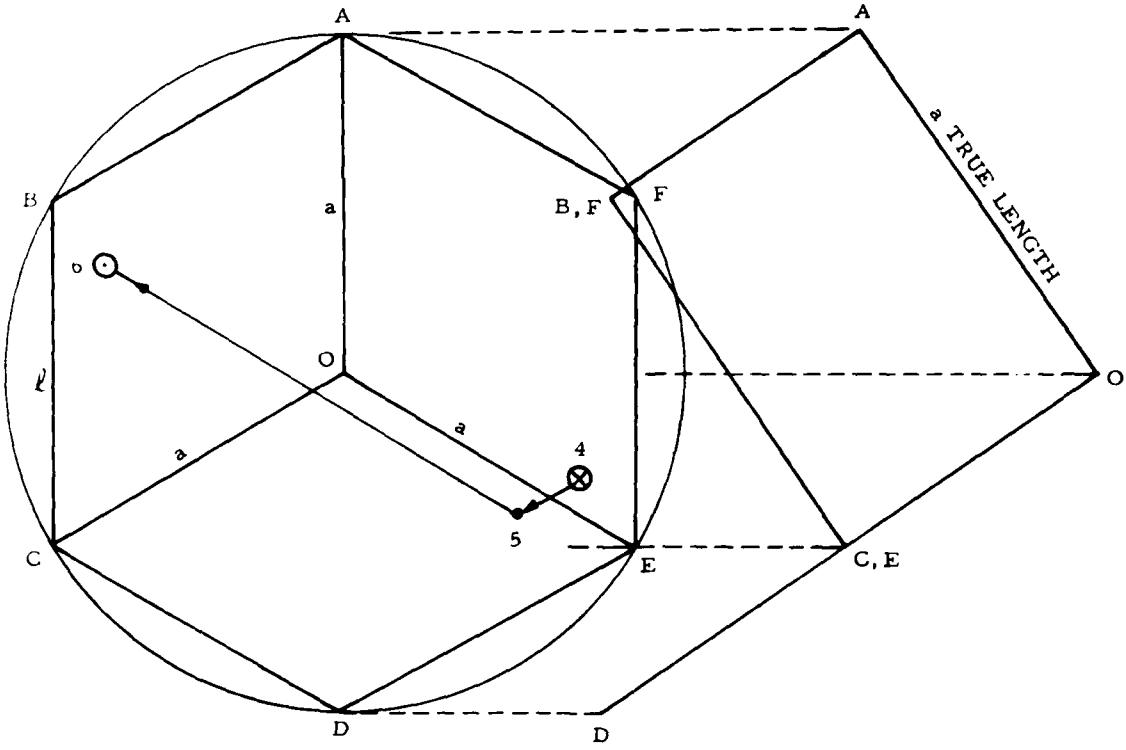
$$S = \text{AREA OF } GHIJKL = \frac{3\sqrt{3}}{2} \left(\frac{2a^2}{9} \right) \quad \ell = \frac{\sqrt{2}}{3} a$$

$$S = \frac{a^2}{\sqrt{3}}$$

$$\text{MAX RADAR CROSS-SECTION } \sigma = \frac{4\pi S^2}{\lambda} = \frac{4\pi a^4}{3\lambda}$$

79-56-5

FIGURE 5. TRIANGULAR CORNER REFLECTOR



S = EFFECTIVE AREA = AREA OF REGULAR HEXAGON ABCDEF

$$S = \text{AREA OF REGULAR HEXAGON OF SIDE LENGTH } l = \frac{3\sqrt{3}}{2} l^2$$

$$S = \text{AREA OF ABCDEF} = \frac{3\sqrt{3}}{2} \left(\sqrt{\frac{2}{3}} a \right)^2 \quad l = \sqrt{\frac{2}{3}} a$$

$$S = \sqrt{3} a^2$$

$$\text{MAX RADAR CROSS-SECTION } \sigma = \frac{4\pi S^2}{\lambda^2} = \frac{12\pi a^4}{\lambda^2}$$

79-56-6

FIGURE 6. **SQUARE CORNER REFLECTOR**

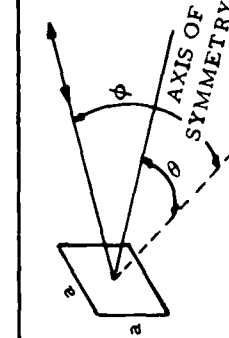
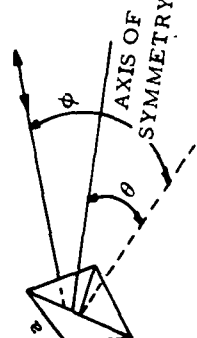
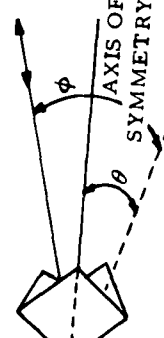
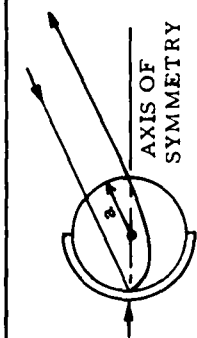
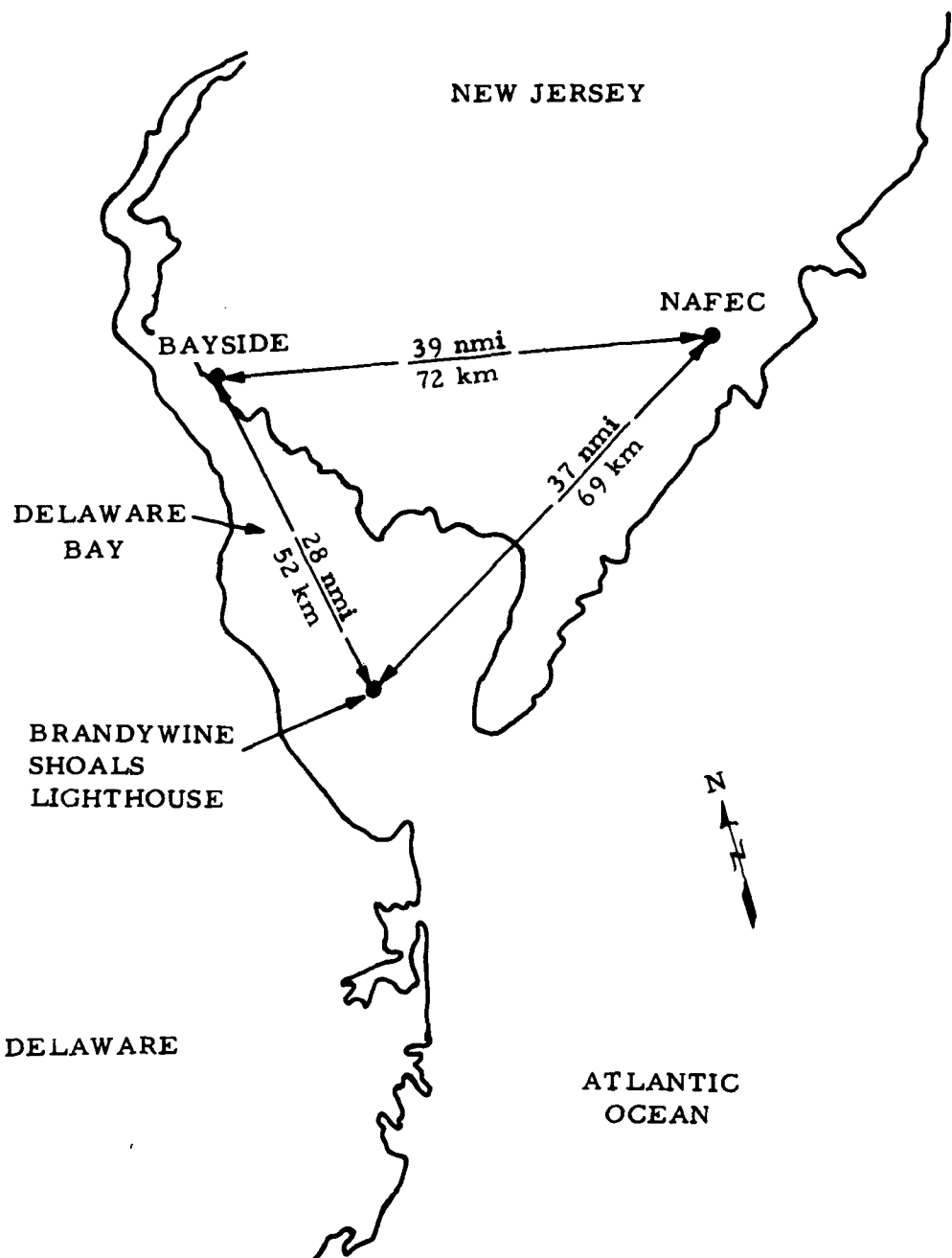
TYPE	DIMENSIONS	EQUIVALENT FLAT PLATE AREA (S)	MAX. RADAR CROSS SECTION (σ)	σ MAX. (M^2) FOR $a=1.5$ m & $\lambda=3.2$ cm
FLAT PLATE		a^2	$\frac{4\pi(a^2)}{\lambda^2}$	62,126
TRIANGULAR CORNER		$\frac{a^2}{\sqrt{3}}$	$\frac{4\pi a^4}{3\lambda^2}$	20,709
SQUARE CORNER		$\sqrt{3} a^2$	$\frac{12\pi a^4}{\lambda^2}$	186,379
LUNEBURG LENS		πa^2	$\frac{4\pi^3 a^4}{\lambda^2}$	613,161

FIGURE 7. SUMMARY OF PASSIVE REFLECTOR CHARACTERISTICS

79-56-7



79-56-8

FIGURE 8. AIRBORNE RADAR APPROACH TEST SITES

ESTATE PLANNING

HISTOGRAMS OF HACCS

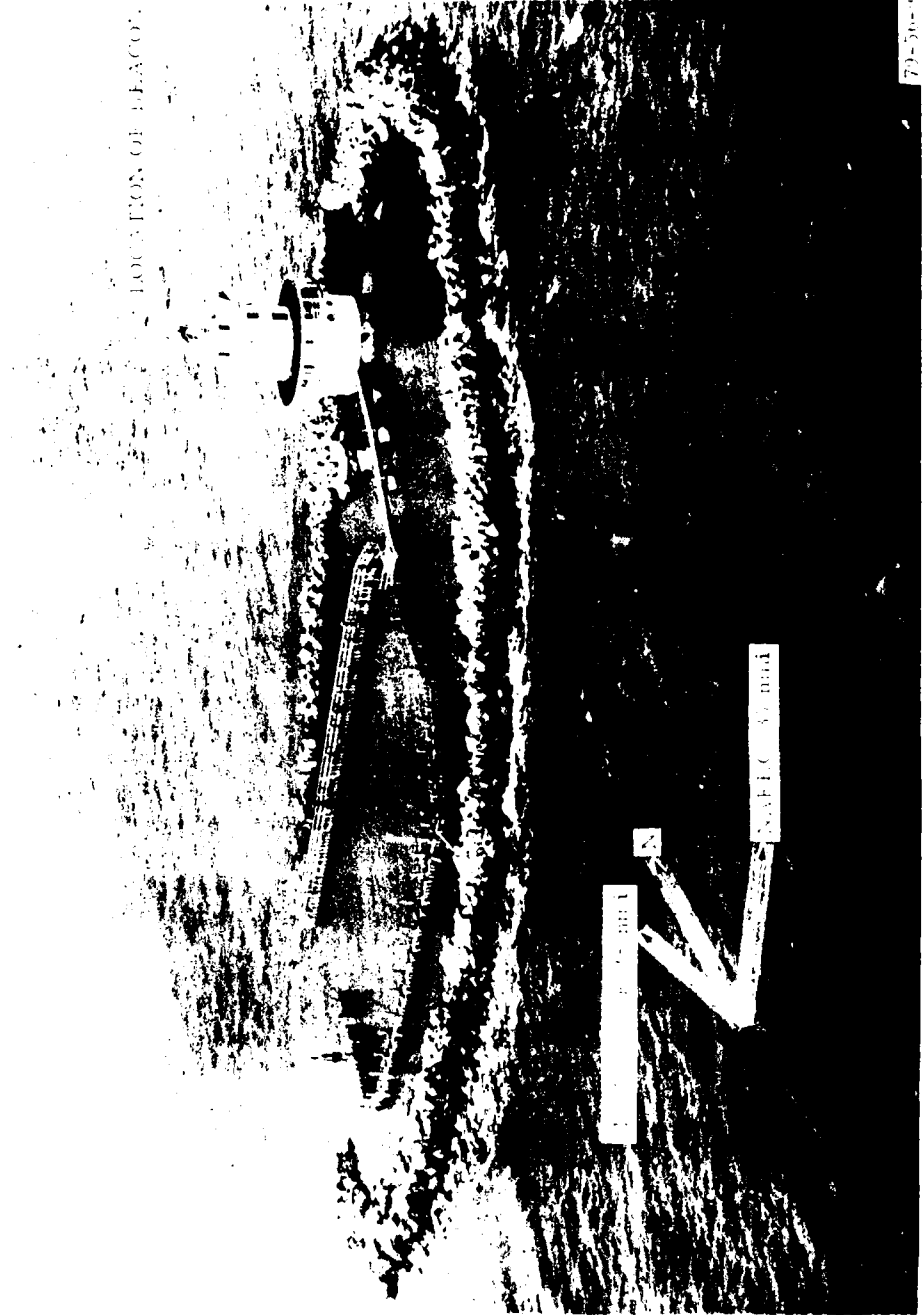


FIGURE 9. BRANDYWINE SHOALS LIGHTHOUSE, OFFSHORE TEST SITE

BAYSIDE, NEW JERSEY

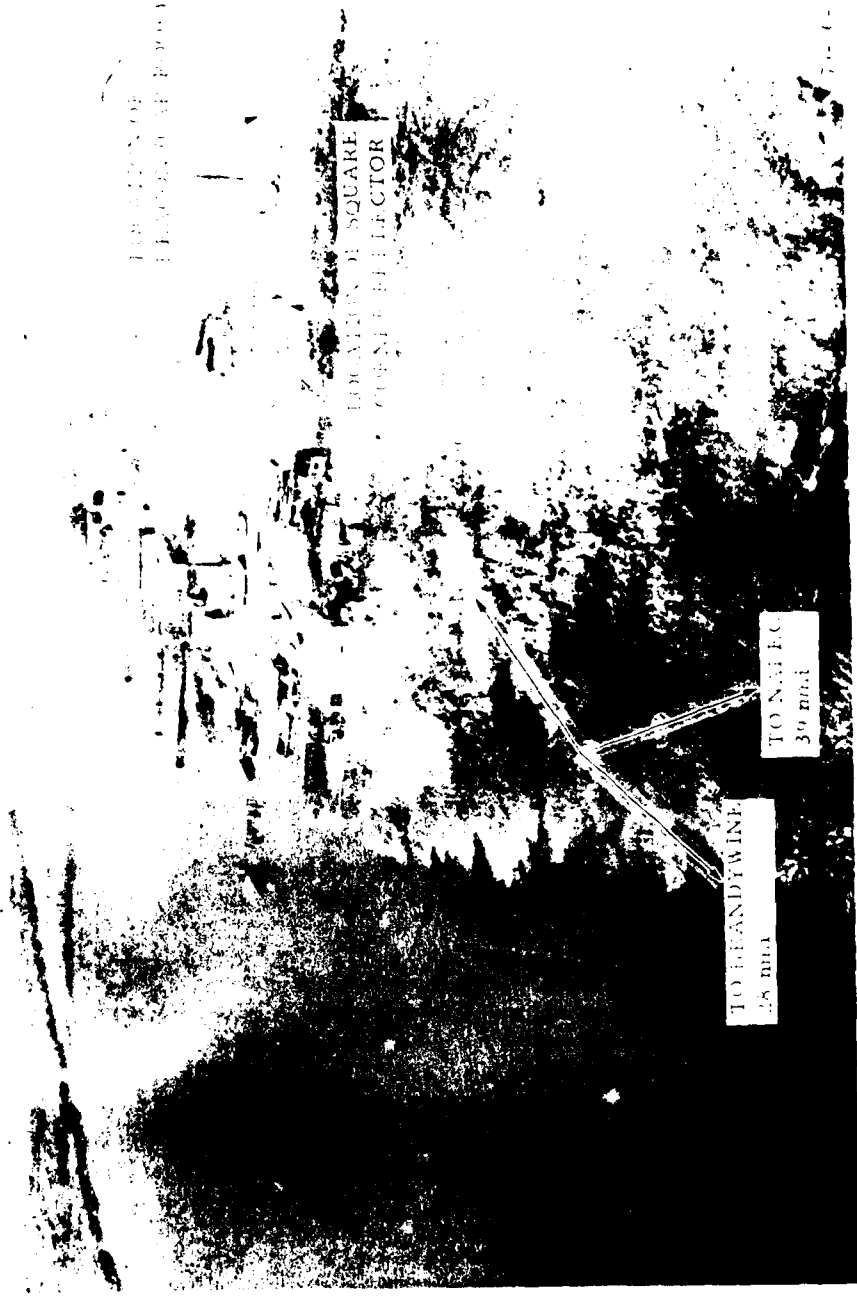
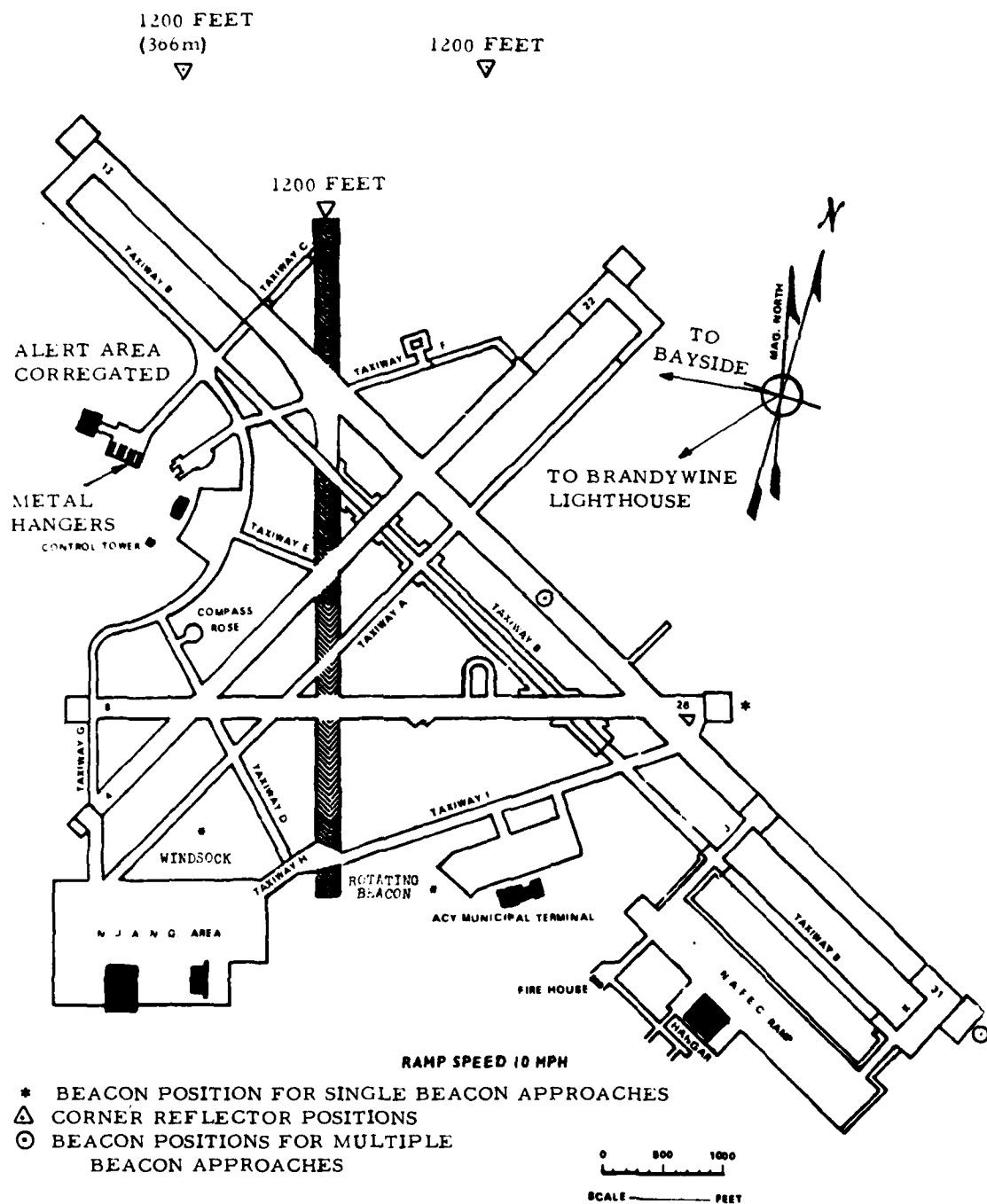


FIGURE 10. BAYSIDE, NEW JERSEY, REMOTE TEST SITE



NAFEC/ATLANTIC CITY AIRPORT, ATLANTIC CITY, NEW JERSEY

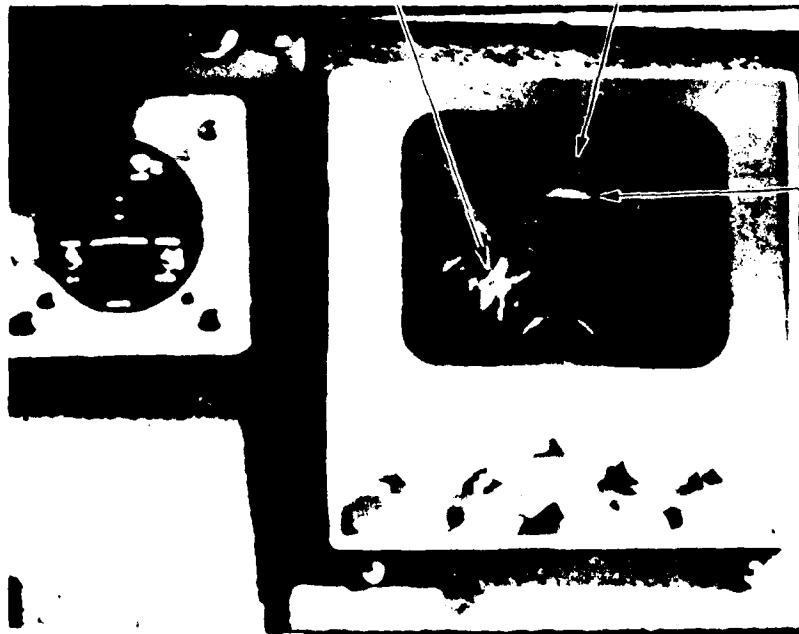
NA FORM 5320-1 (5-75)

79-56-11

FIGURE 11. NAFEC AIRPORT TEST SITE

BOATYARD ISLANDS

BAYSIDE
BUILDINGS



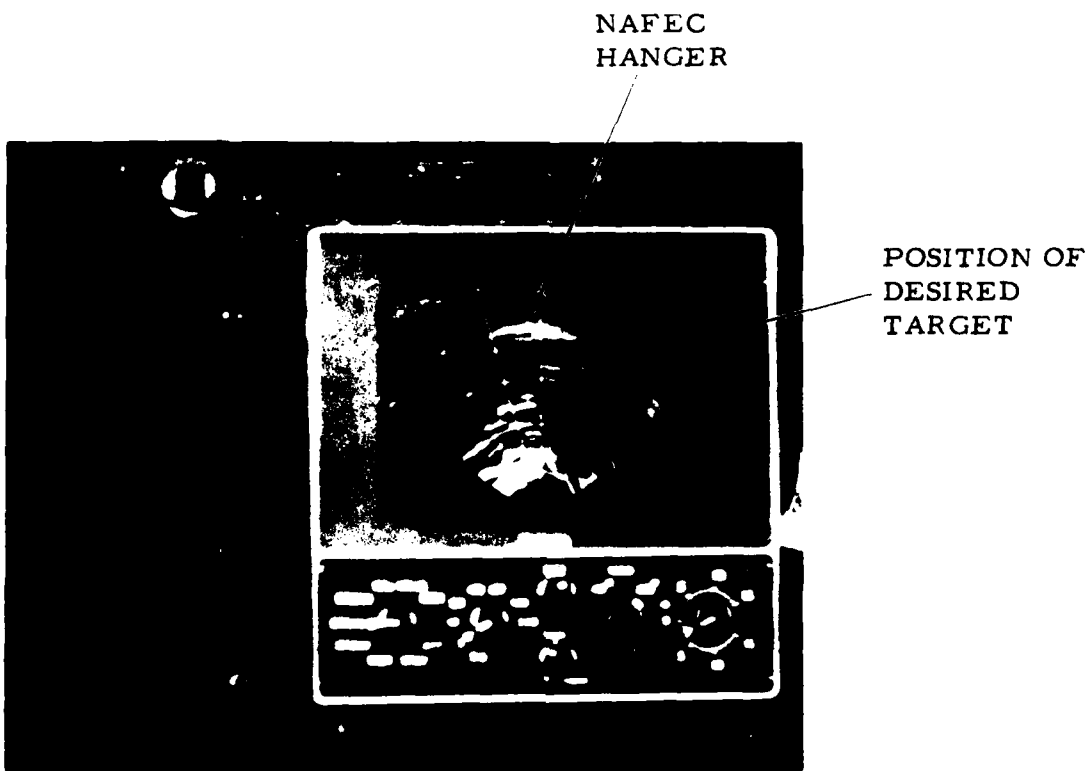
8/4/78
BAYSIDE, N.J. FROM DIRECTION OF NAFEC

RANGE \approx 3 1/2 nmi
ALTITUDE \approx 500 FEET AGL.

SINGLE LARGE CORNER REFLECTOR

79-56-12

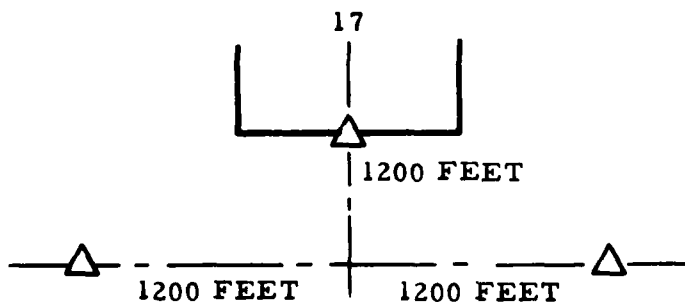
FIGURE 12. RADAR DISPLAY AT BAYSIDE TEST AREA



7/26/78
NAFEC AIRPORT, N.J. FROM DUE N.

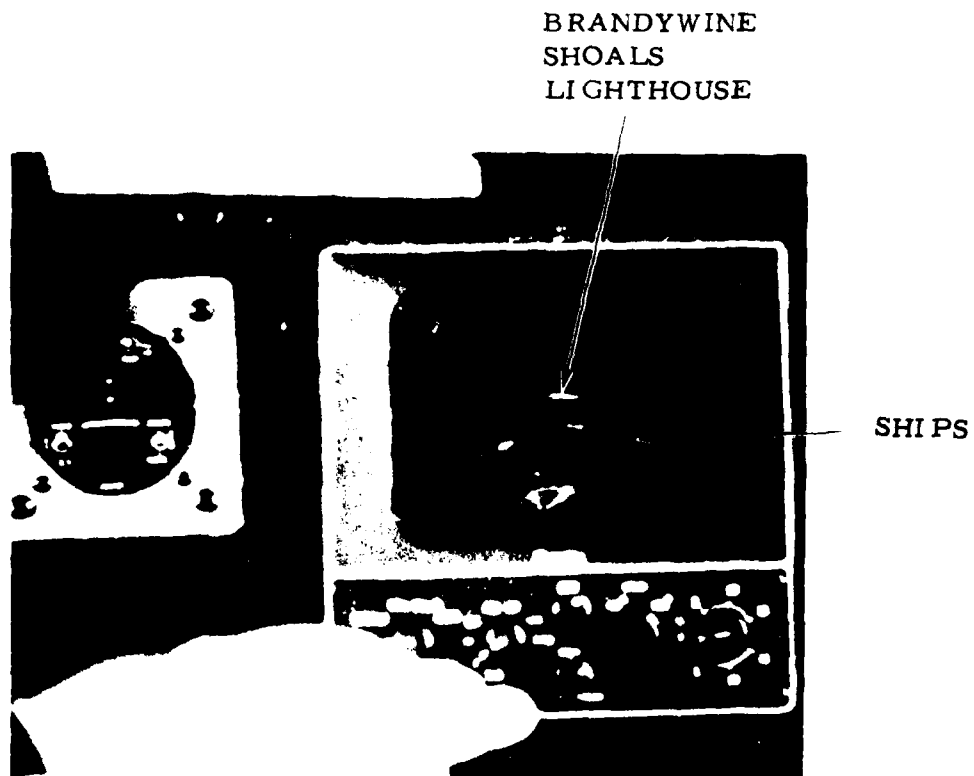
RANGE≈3 nmi
ALTITUDE≈ 500 FEET AGL

SINGLE LARGE REFLECTOR ON RUNWAY THRESHOLD
TWO SMALL REFLECTORS IN THIS PATTERN



79-56-13

FIGURE 13. RADAR DISPLAY AT NAFEC TEST AREA



8/4/78

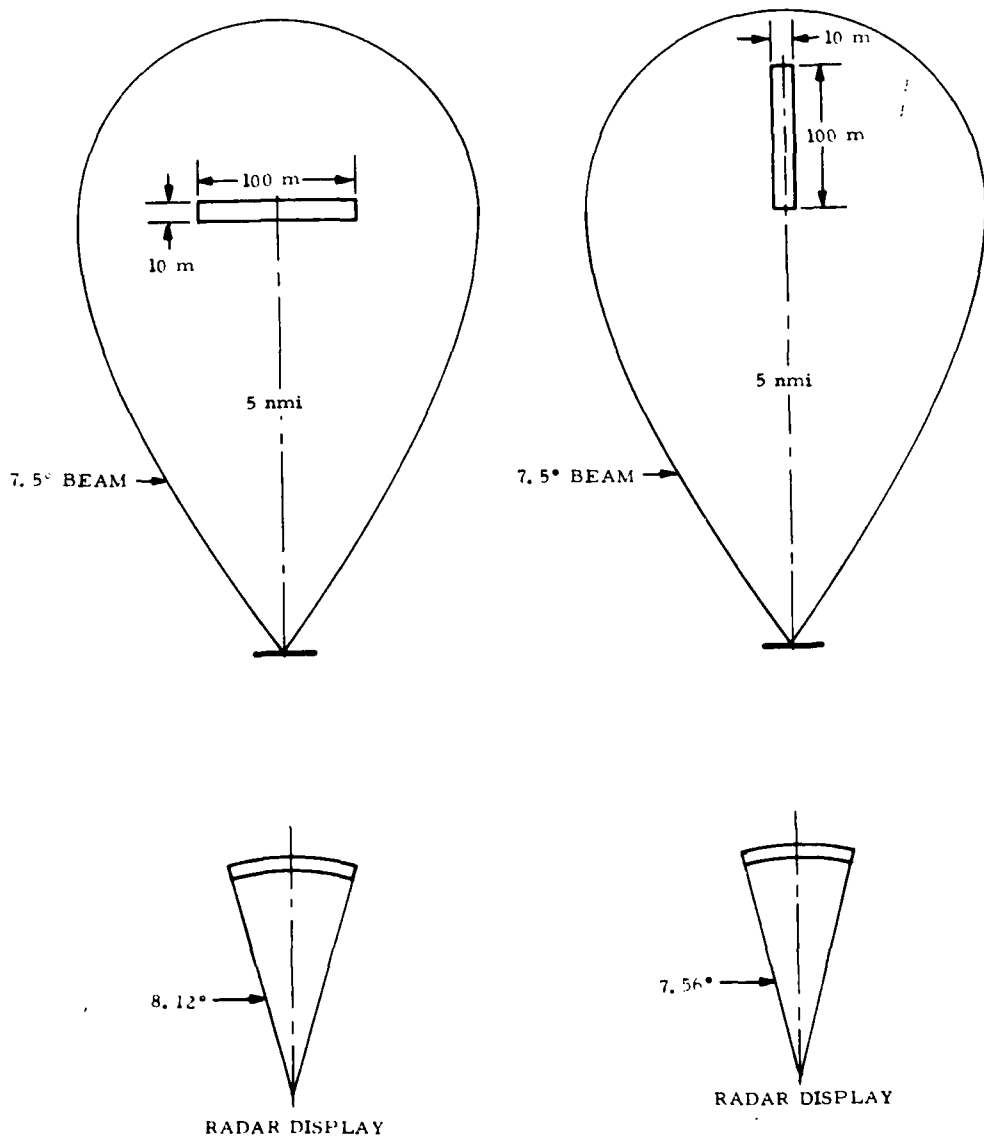
BRANDYWINE SHOALS LIGHTHOUSE FROM THE DIRECTION
OF BAYSIDE, N.J.

RANGE \approx 3 nmi
ALTITUDE \approx 500 FEET AGL

NO PASSIVE ENHANCEMENT

79-56-14

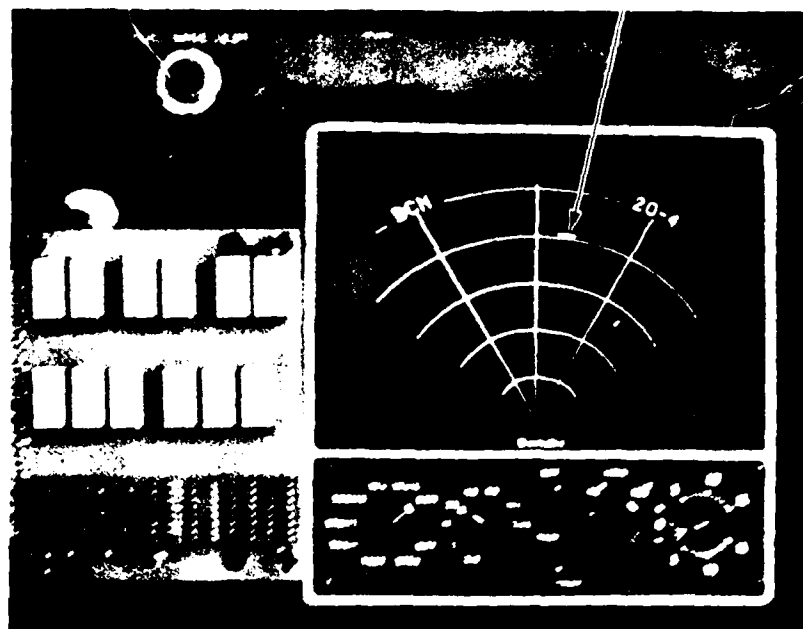
FIGURE 14. RADAR DISPLAY AT BRANDYWINE SHOALS LIGHTHOUSE



79-56-15

FIGURE 15. COMPARISON OF VERTICAL AND HORIZONTAL RADAR TARGETS

BEACON
RETURN



11/14/78

BAYSIDE, N.J. FROM DIRECTION OF NAFEC

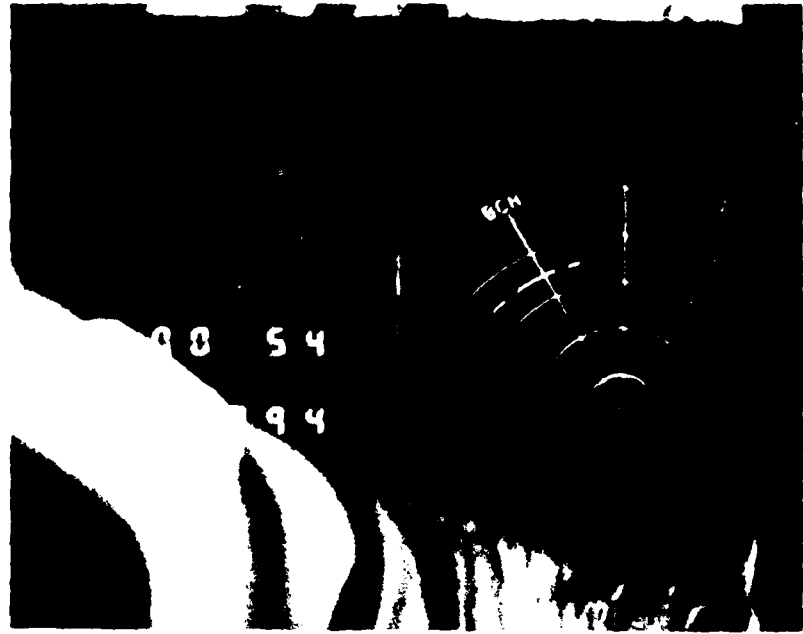
RANGE \approx 16 nmi

ALTITUDE \approx 1000 FEET AGL

SINGLE TRANSPONDER NEAR GROUND LEVEL

79-56-16

FIGURE 16. RADAR DISPLAY AT BAYSIDE TEST AREA, SINGLE RADAR BEACON



12/14/78
NAFEC AIRPORT

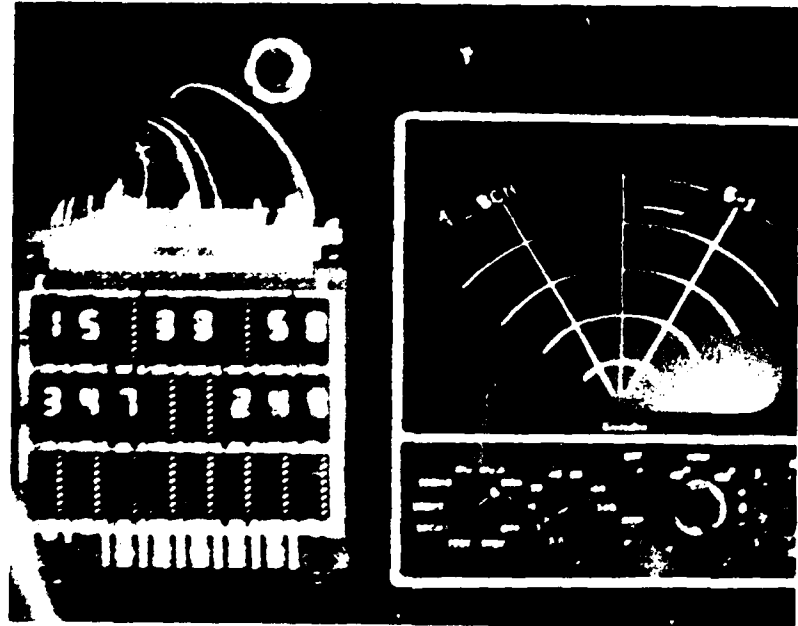
RANGE \approx 7 nmi
ALTITUDE \approx 500 FEET AGL

SINGLE TRANSPONDER AT GROUND LEVEL

TOO HIGH A GAIN SETTING ALLOWING DISPLAY
OF BEACON RETURNS TRIGGERED BY SIDELINES

79-56-17

FIGURE 17. RADAR DISPLAY SHOWING MULTIPLE BEACON RETURNS DUE TO
SIDELOBE TRIGGERING - HIGH RADAR DISPLAY GAIN SETTING



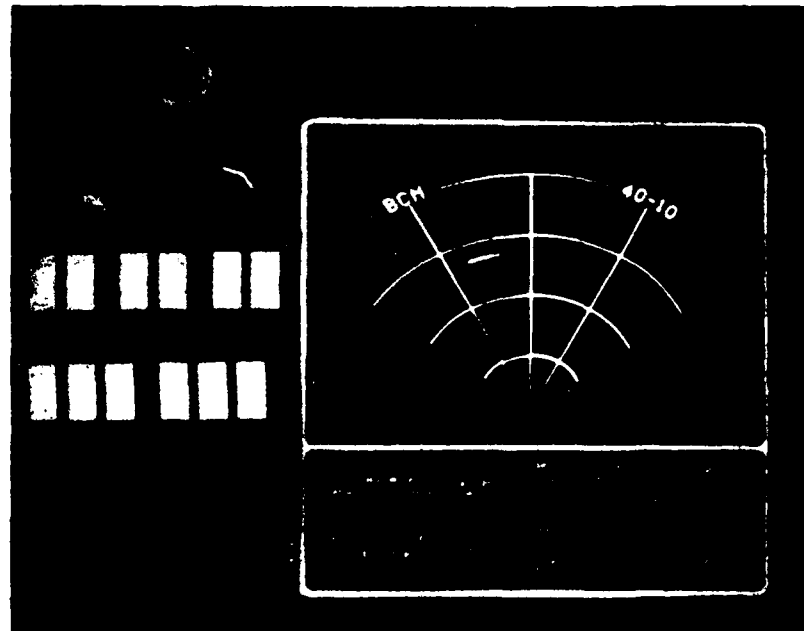
12/13/79
NAFEC AIRPORT

RANGE \approx 4.3 nmi
ALTITUDE \approx 500 FEET AGL

SINGLE TRANSPONDER AT GROUND LEVEL

79-56-18

FIGURE 18. RADAR DISPLAY AT NAFEC TEST AREA, SINGLE RADAR BEACON



11/14/78

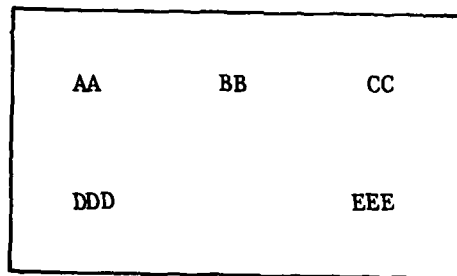
BRANDYWINE SHOALS LIGHTHOUSE FROM DIRECTION
OF BAYSIDE, N. J.

RANGE \approx 28 nmi
ALTITUDE \approx 1000 FEET AGL

SINGLE TRANSPONDER MOUNTED ON LIGHTHOUSE

79-56-19

FIGURE 19. RADAR DISPLAY AT BRANDYWINE SHOALS LIGHTHOUSE, RADAR BEACON ON LIGHTHOUSE



AA		Hours
BB	Time of Day	Minutes
CC		Seconds
DDD	Julian date i.e.: 1 = Jan 1 365 = Dec 31	
EEE	Aircraft Magnetic Heading	

FIGURE 20. DIGITAL DISPLAY UNIT

